

Simulation of Ice-Structure Interaction with CZM-Elements

Hauke Herrnring, Leon Kellner, Jan M. Kubiczek, Sören Ehlers

Technische Universität Hamburg

1 Introduction

Simulations of ice interaction scenarios are not as reliable as desired. The reason for this shortcoming is often the limitation of the ice model. Whereas steel models for the ship or the structure are well established, there is no model available for ice that can capture the complete interaction process. This is due to many reasons, such as complex ice properties. Here, the focus is on the brittle fracture behavior of ice. Cohesive zone elements are suggested to model fracture whereas standard finite elements reflect the bulk material. A general procedure to determine model parameters for the cohesive zone model is outlined.

The motivation stems from the retreat of sea ice and increased economic interest in the arctic regions [1] as well as the development of offshore wind power, e.g. in the Baltic Sea [2]. The consequence is an increasing number of ship operations and offshore activities in ice-covered waters. Ice-loads are significant for the design of maritime structures operating in these waters. Currently, the dimensioning process against ice loads is mostly based on empirical formulas [3, 4]. They are used to estimate upper limits of static global loads, but they don't give local loads and the structure is modeled as rigid. Dynamic behavior and ice interaction are neglected.

On the other hand it is important to include interaction in the model since this can influence the outcome, e.g. forces [5]. Numerical simulations, e.g. FEM, make it possible to model the structure as deformable and therefore consider interaction between ice and structure. It is also straightforward to test different ice and structure geometries. Moreover, they give higher resolution results and can be used in local load driven design. Overall, such simulations are a desirable tool for the design of maritime structures. However, the accuracy of these simulations is often limited by the ice model. This includes the material model, e.g. viscoelastic, as well as fracture behavior.

In this research, the focus is on modeling the fracture behavior of ice under high loading rates, i.e. in brittle failure modes. This kind of behavior is also expected to show in ice impacts with ships. Currently, this is often done by erosion of solid elements in the contact surface, e.g. [6]. Because the contact surface in ice interaction is dominated by compression, element erosion leads to unphysical results. The applied numerical method has to preserve the volume and allow for an arbitrary fracture path. Furthermore, the mass transport of broken ice pieces in the contact surface and spalling of bigger ice spalls must be represented by the model. Lastly, multiple, branching cracks need to be captured by the model within reasonable computation time. According to these requirements, the cohesive zone method (CZM) is applied.

Several authors use the CZM to simulate brittle ice problems [7–10]. However, the model parameters are often tuned for a specific application. It is not clear how to derive parameters for a different purpose and what the limitation of the original model and its parameters are. Consequently, the general applicability of these approaches is limited. Here, a general procedure is given to calibrate parameters for a bilinear cohesive zone model based on a range of different experiments.

As an exemplary application, the CZM is used to simulate an ice drop test in the laboratory. This way, high loading rates and elastic brittle behavior is ensured. Creep is negligible. Furthermore, the conditions during a laboratory test are controllable and hence known. This is seen as a first step toward ice models for full scale scenarios.

2 The Cohesive Zone Method and its implementation

The cohesive zone method was originally proposed in the 1960's, see e.g. [11, 12]. A comprehensive Introduction to the cohesive zone method is given in [13]. The cohesive zone handles the process

zone ahead of a crack tip. In this zone traction between two virtual surfaces exists. The traction is a function of the displacement between the surfaces, the traction-separation law (TSL). The cohesive element fails when the separation reaches a critical value. The maximum traction and critical separation of a TSL are material parameters. Moreover, various shapes of TSL exist to model different types of fracture, e.g. ductile or brittle fracture. Also, TSL can incorporate damage, i.e. the separation process is irreversible. In this case the function does not follow the original path back to the origin once the maximum traction is reached. Instead, the element stiffness is permanently decreased, and the path is a straight line from the current state to the origin.

Here, a bilinear TSL with damage is used since the ice is presumed to show brittle behavior. All inelastic deformation is assumed to be a separation of crack faces. Currently, the cohesive mixed mode material model (**MAT_138**) is used. It was developed to simulate delamination in laminated composites [14]. The key input parameters are traction, maximum separation and the energy release rate. Delamination initiation is predicted using a quadratic failure criterion:

$$\sqrt{\left(\frac{\sigma_z}{T}\right)^2 + \left(\frac{\tau_{xz}}{S}\right)^2 + \left(\frac{\tau_{yz}}{S}\right)^2} = 1; \sigma_z > 0, \text{ i.e. tension} \quad (1)$$

$$\sqrt{\left(\frac{\tau_{xz}}{S}\right)^2 + \left(\frac{\tau_{yz}}{S}\right)^2} = 1; \sigma_z \leq 0, \text{ i.e. compression} \quad (2)$$

Where σ and τ are normal and shear stresses, respectively and T and S are the maximum tractions the element can sustain without being damaged. Delamination propagation is computed through the interaction of energy release rates:

$$\left(\frac{G_I}{G_{Ic}}\right)^\alpha + \left(\frac{G_{II}}{G_{IIc}}\right)^\alpha = 1 \quad (3)$$

In the model, zero thickness cohesive elements are put in between all faces of the bulk elements (Fig. 2.). Tetrahedron elements are used instead of hexahedrons to allow for a somewhat arbitrary crack pathing. Overall, implementing cohesive elements into a model is straightforward. However, it introduces several issues which need to be addressed.

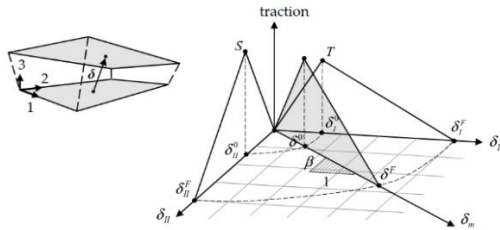


Fig.1: Traction separation law for MAT138 [15]

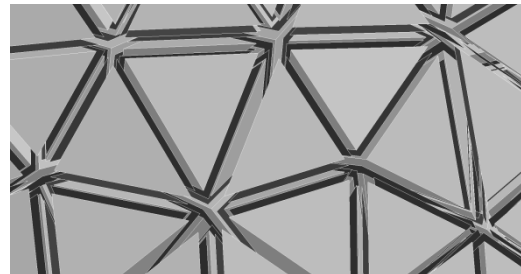


Fig.2: Detail of a Cohesive Zone Model (grey: shrunk solid elements, black: CZM elements)

2.1 Added Mass of the CZM Element

Cohesive elements are not massless. The addition of cohesive elements to an existing FE model increases the overall mass of the modeled body. An incorrect mass leads to unphysical results for energy limited problems. The total mass m of a model with cohesive elements is defined as the sum of the mass of solid elements m_s and cohesive elements m_{CZM} :

$$m = m_s + m_{CZM} \quad (4)$$

In order to compensate for the additional mass of the cohesive elements, it is proposed to reduce the mass of the solid element and adapt the mass of the cohesive element accordingly.

The following relationships are representative for a single solid element with a volume V_s and a surface area S_s , surrounded by cohesive elements. The real density of ice is ρ_{real} . The adapted densities of the solid elements ρ'_s and cohesive elements ρ'_{CZM} are calculated as:

$$m = \rho_{real} V_s \quad (5)$$

$$m_S = \rho'_S V_S \quad (6)$$

$$m_{CZM} = \frac{1}{2} S_S \rho'_{CZM} t_{CZM} \quad (7)$$

$$f_m = \frac{m_{CZM}}{m} \quad (8)$$

The artificial thickness of the cohesive elements t_{CZM} is one unit of length (e.g. in SI units 1m). A mass ratio f_m between cohesive and solid elements is introduced. The density for the cohesive elements results from Equation 5, 7 and 8:

$$\rho'_{CZM} = 2f_m \frac{\rho_{real} V_S}{S_S t_{CZM}} \quad (9)$$

Correspondingly, for a mesh of cubes or tetrahedrons with an constant edge length L_S , the following relations can be obtained by:

$$\rho'_{CZM,Cube} = 2f_m \frac{\rho_{real} L_S^3}{6L_S^2 t_{CZM}} = \frac{1}{3} f_m \frac{\rho_{real} L_S}{t_{CZM}} \quad (10)$$

$$\rho'_{CZM,Tet} = 2f_m \frac{\rho_{real} \frac{\sqrt{2}}{12} L_S^3}{\sqrt{3} L_S^2 t_{CZM}} = \frac{1}{6} \sqrt{\frac{2}{3}} f_m \frac{\rho_{real} L_S}{t_{CZM}} \quad (11)$$

The corrected density for the solid elements is determined by:

$$\rho'_S = (1 - f_m) \rho_{real} \quad (12)$$

We recommend a value for f_m of 0.5. In addition, the density of the cohesive elements only depends on the element size L_S . All other quantities are physically determined.

2.2 Artificial compliance

Using zero thickness cohesive elements with a bilinear TSL introduces artificial compliance to the model [16]. A straightforward solution is to use a very high initial stiffness, i.e. slope of the TSL. This approach is limited since the time step is controlled by the elastic modulus of the material. Element size also influences artificial compliance [16]. To determine the correct elastic moduli for the elements a series of springs is assumed. The spring stiffness of a rectangular solid element k_S and cohesive element k_{CZM} is defined as:

$$k_S = \frac{E_S A_S}{L_S} \quad (13)$$

$$k_{CZM} = \frac{E_{CZM} A_{CZM}}{t_{CZM}} \quad (14)$$

The cross-section area of the cohesive elements A_{CZM} and the solid elements A_S can be assumed to be equal. Furthermore, the elastic moduli from the solid and cohesive element E_S and E_{CZM} and also the element lengths L_S and t_{CZM} are required. t_{CZM} is an artificial thickness with a value of one. A stiffness ratio f_k is defined:

$$f_k = \frac{k_{CZM}}{k_S} \quad (15)$$

The left side of Equation 16 represents the series of solid elements without CZM elements. The right side consists of the sums of spring stiffnesses of cohesive and solid elements. To maintain the original overall stiffness, the artificial compliance introduced by the CZM elements has to be compensated by increasing the spring stiffness of the solid elements k'_S .

$$\sum \frac{1}{k_S} = \sum \frac{1}{k'_S} + \sum \frac{1}{k_{CZM}} \quad (16)$$

Introducing the number of solid n_S and cohesive n_{CZM} elements into Equation 16:

$$\frac{n_S}{k_S} = \frac{n_S}{k'_S} + \frac{n_{CZM}}{k_{CZM}} \quad (17)$$

We assume $n_{czm} = n_S - 1$, f_k as well as $k'_S = E'_S A_S / L_S$, then the adapted elastic modulus E'_S of the solid elements is

$$E'_S = E_S \left(1 - \frac{1}{f_k} + \frac{1}{n_S f_k} \right)^{-1} \quad (18)$$

Increasing the number of elements leads to:

$$\lim_{n_s \rightarrow \infty} : E'_s = E_s \left(1 - \frac{1}{f_k}\right)^{-1} \quad (19)$$

The corresponding stiffness for the CZM elements is defined according to the equations (13,14 and 15) as follows:

$$E_{CZM} = \frac{f_k t_{CZM} E_s}{L_s} \quad (20)$$

For tetrahedrons, Equation 20 is adjusted by simulations of a simple block in tension. The result is:

$$E_{CZM} = \frac{f_k t_{CZM} E_s}{0.5 L_s} \quad (21)$$

To determine a reasonable value for f_k , the graph in Figure 3 is used. It indicates the increase of the solid element stiffness, in dependency of the stiffness ratio f_k , which is necessary to compensate the artificial compliance. In order to limit the necessary increase in the stiffness of the solid elements, a value of $f_k = 10$ is recommended. At first glance, a higher value for f_k seems favorable, as this improves the convergence behavior of the equation 18. But, as mentioned, this also decreases time step size. With $f_k = 10$ the deviation in tension or compression in case of 10 elements is around 1% against the limit of the function 19.

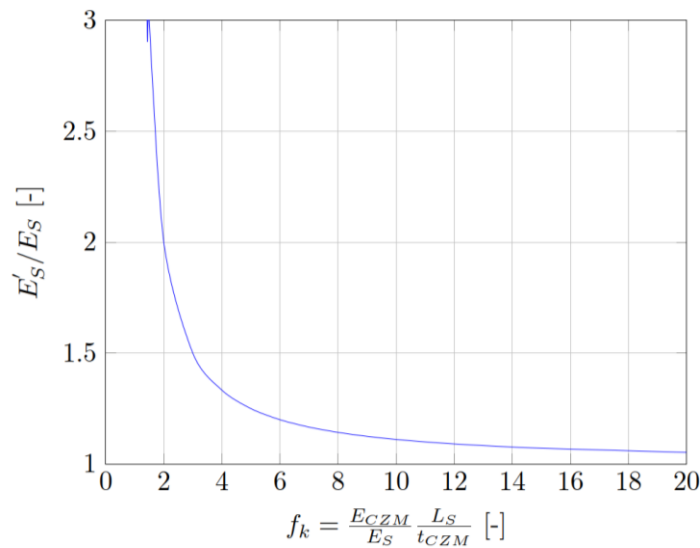


Fig.3: Increase of stiffness of the solid elements depending on the stiffness ratio f_k

The approach was validated by simulating a simple block with a dimension of 1 m by 1 m meshed with hexahedrons and tetrahedrons with edge length of 0.1 m. The block was loaded under compression, tension and shear with a final deformation of 0.1 mm each. The resulting stresses are shown in Table 1. The deviations were small. These stiffness validation simulations were also conducted successfully for different element sizes. Adding a segment based `*CONTACT_AUTOMATIC_SINGLE_SURFACE` contact algorithm (`SOFT=2`, `DEPTH=5`) barely affected the results. This contact algorithm turned out to be necessary for later, more complex simulations.

Table 1: Comparison of solid element stresses for the validation of stiffnesses

	Without CZM Pa	Hex CZM Pa	Tet CZM Pa	Tet CZM contact Pa
Tension (z-Stress)	9.00E+05	9.09E+05	9.00E+05	9.10E+05
Compression (z-Stress)	-9.00E+05	-9.09E+05	-9.01E+05	-9.15E+05
Shear (vM)	5.77E+05	5.81E+05	5.75E+05	5.81E+00

2.3 Number of elements in the process zone

Another issue is the number of elements in the process zone necessary to reflect realistic fracture initiation and propagation. First, the length of the cohesive zone has to be estimated. This can be done with several formulas, which are typically given for either plane stress or plane strain conditions. The cohesive zone length varies significantly for different formulas. Here, it is estimated for brittle fracture and plane strain according to [17]

$$l_{cz} = \frac{9\pi}{32} \left(\frac{E}{1-\nu^2} \right) \frac{G}{\tau_{max}^2} \quad (22)$$

Second, the length is compared to the average element edge length. The minimum number of elements required in the cohesive zone is subject of ongoing discussion, and literature values range from two to more than 10 elements. It is also possible to use a bigger failure separation value, as long as the energy release rate is constant. In other words, the TSL can be flattened to achieve a sufficient number of elements in the cohesive zone [18]. According to Equation (22) and an element edge length of 10 to 15 mm, the number of elements in the process zone is approximately 2-10, depending on the separation mode. It has to be kept in mind that the plane strain assumption is not valid in many cases.

2.4 Delamination initiation

Lastly, delamination initiation is independent of compressive stress ($\sigma_z \leq 0$) for laminated composites, Equation (2). This is not the case for ice. The ratio of hydrostatic stress to von Mises stress influences the failure mechanism [19]. If the ratio exceeds a value of approximately 10, ice is unlikely to fail during experiments. However, this phenomenon is expected to have little influence on the current simulations, since the ice is not laterally confined.

3 Material parameter identification based on small scale experiments

To show the principle applicability of the CZM for ice related problems and determining the material parameters a series of small scale experiments were simulated. Literature and own measurement results were available for comparison to the simulations. The following simulations were conducted: Tensile test, shear test, compression test, CTOD test and a tensile splitting test.

All simulations were performed with the same basic settings. Tetrahedron elements were used to allow random crack propagation. Only the CTOD test was discretized with hexahedrons, because of the known fracture path. The average edge length of the elements of the ice models was 10 mm. Due to hourglassing problems of the hexahedron solid elements a fully integrated element type `etype=-1` was used. For the tetrahedron elements the element type 13 was chosen. The cohesive elements were either of type 19 or 21.

Depending on the complexity of the model, the meshing was performed with external programs or in LS-PrePost. In order to maintain uniform stiffness properties, the element size may change only slightly. Symmetric planes have to be avoided. In general, the cohesive elements were inserted into the existing mesh with LS-PrePost. The time step size was generally reduced by `TSSFAC=0.45` in `*CONTROL_TIMESTEP`. The default critical time step size estimation of `ICOH=0` in `*CONTROL_SOLID` is chosen. Without reducing the time step size instabilities are observed.


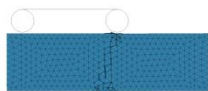
To avoid a penetration of the solid elements after the erosion of the cohesive elements a segment based `*CONTACT_AUTOMATIC_SINGLE_SURFACE` algorithm was applied. The segment set consists of all solid faces of the ice part. To obtain a stable contact behavior the additional contact options of card A `soft=2` and `depth=5` were selected. A constant friction coefficient of 0.01 for the contact between ice and ice was assumed. The material properties of ice are generally affected by defects and imperfections. To model the resulting inhomogeneity of the material behavior one percent of the cohesive elements was randomly deleted.

The material properties for solid ice elements and the cohesive elements were obtained by values given in literature and parameter identification with simulations of the presented tests. First the tensile test and the shear test were simulated. An energy release rate for ice of 4 J/m² is assumed. The value is calculated according to the fracture toughness of 0.2 MPa/√m given by Palmer [20]. Measurements for mode II are not available. Therefore, the energy release rate of mode I is also adopted for mode II.

The assumed value of 4 J/m² seems reasonable, because higher values for the energy release rate do not result in brittle fracture behavior of ice in the simulations. In case of higher energy release rates, the force after fracture does not drop immediately. This result is in line with fracture toughness experiments in small-scale [21, 22].

Before the required material parameters for the cohesive elements can be determined, the material model for the solid elements must be selected. An elastic material model for the solid elements is used. The density of the solid elements is reduced by half to 450 kg/m³. The elastic modulus is assumed to be 9 · 10⁹ Pa and corrected with formula 19. The Poisson's ratio is assumed to be 0.35. Basic material parameters for ice are given for instance in [23, 24]. For the complete description of the model only the peak traction in tension and shear are missing. These parameters are identified by simulating the shear and tensile test with different parameter sets. The results for the shear and tensile test are presented in Table 2.

Table 2: Selected small-scale simulations

Test type	Model	Source of data	Ice type	Target value	Simulation
Tensile		Currier et al. [25]	Distilled water	1 MPa = 6.5 kN Grain size ~ 2.3 mm	5.93 kN
Shear		Frederking et al. [26]	Columnar-grained fresh-water ice	5 kN	7 kN

The final parameter set is given in Table 3. A lower limit for shear strength is half the tensile strength. This relation is given by the Mohr-Circle. A compromise between tension and shear strength is chosen. The crack patterns and forces of the simulations agree reasonably well with the experiments. With the obtained parameters, a compression-, tensile splitting and CTOD test were also simulated successfully (compared to own measurements and [27]).

Table 3: Material parameters for the cohesive and solid ice elements

Description	Symbol / variable	Value	Source
Cohesive elements, MAT 138			
Density	RO	Mesh dependent	Equation (10) or (11)
Stiffnesses	EN=ET	Mesh dependent	Equation (20) or (21)
Energy release rates	GIC=GIIC	4 J/m ²	Fracture toughness [20]
Normal peak traction	T	1.2 MPa	Simulation
Tangential peak traction	S	0.6 MPa	Simulation
Ultimate displacements	UND, UTD	UND=6.67e-6 mm, UTD=1.33e-5 mm	Calculated from GIC and T
Solid elements, MAT ELASTIC			
Density	RO	0.5*900 kg/m ³ = 450 kg/m ³	Equation (12), own measurements
Poisson's ratio	PR	0.35	[28]
Young's modulus	E	1e10 Pa	Equation (19) with f_k=10

4 Drop tests

The CZM was also applied to more complex ship-ice related problems. Two experiments of a drop test series were simulated. Cylindrical ice specimens with a diameter of 200 mm and a conical tip with an angle of 30° were used for impacting rigid plates and deformable aluminum panels (5083-H116 alloy). The drop mass was 224 kg and impact velocity of 1.5 m/s. A detailed description of the experiments can be found in [29]. Both tests, against a rigid and deformable plate, were simulated.

The previously determined parameters for the cohesive elements have been adopted. The element size was adjusted to 0.015 m to reduce computation time. Preliminary simulation runs showed that if kinetic energy could not be absorbed, the majority of CZ elements instantly failed. This resulted in explosion-like behavior of the model. As a remedy, the coefficient of friction was increased from 0.01 to 0.25, which lead to more realistic spalling behavior. This friction coefficient is unphysically high for flat surfaces and high loading rates [30]. However, the true friction conditions are not known. Rough surfaces or recrystallization of the crack may increase the coefficient. 0

The results of the simulation of the drop test against a quasi-rigid plate are shown in Figures 4 and 6. Fracturing of the ice specimen was initiated. The kinetic energy was converted into friction and fracture energy during impact. The fracture pattern was comparable to the experiment. However, the simulated impact force was five times higher than measured. The deceleration of the specimen was too fast compared to the experiment. Lastly, the simulation results did not show a line like pressure distribution. This is typically expected from brittle ice structure interaction.

The results of the simulation of the drop test against a deformable plate are shown in Figures 5 and 7. As in the experiment, no splintering of the ice sample was observed in the simulation. Only few cohesive elements in the contact zone were eroded. The force was mainly limited by the plastic deformation of the aluminum panel. The peak force was around 28 kN, which is a bit higher than in the experiment. The simulation matches the force curve of the experiment.

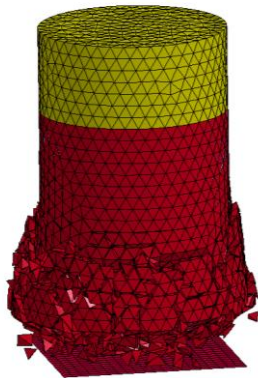


Fig.4: Drop test with 1,5 m/s against a quasi-rigid panel

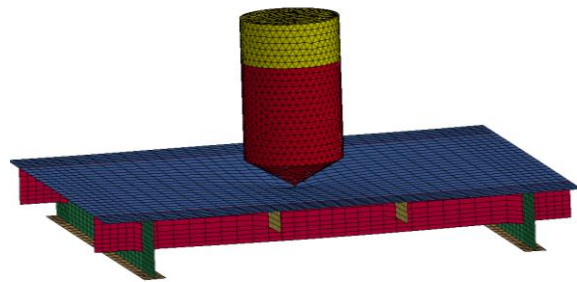


Fig.5: Drop test with 1,5 m/s against a deformable aluminum panel

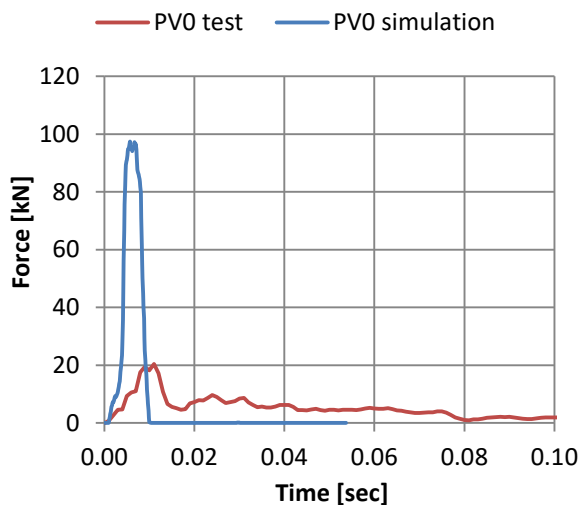


Fig.6: Comparison of measured und simulated contact forces for the quasi-rigid panel

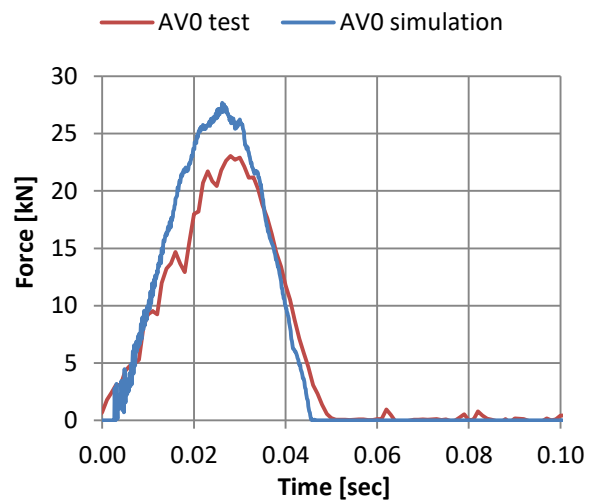


Fig.7: Comparison of measured und simulated contact forces for the deformable aluminum panel

Although the results are satisfactory, some open questions remain, particularly for the simulation with a rigid contact plate. It appears that in the rigid case the forces are limited due to the ice fracturing and crushing behavior. These processes can only be simulated to a limited extent. A different behavior is observed in the deformable plate simulation. In that case the contact forces are dominated by the plastic and elastic deformation of the aluminum panel.

The CZ simulations also showed mesh dependence. For example, the simulation results change significantly when symmetry planes are introduced into the model. In addition, an interaction between the contact algorithm and the CZ elements in compression was found. The single surface contact algorithm prevents the solid elements from penetrating each other. However, it does so even if the CZ element between two solid elements has not been deleted yet and introduces a restoring force at the same time. The resulting contact force via the friction algorithm reduces the shear stress acting in the CZ element. This could be the main reason for the strong dependence on the coefficient of friction.

5 Discussion and Outlook

The CZM is a good method for predicting academic problems dominated by a single crack. The complexity increases for continuous crushing problems with multiple, interacting cracks; energy dissipation and continuum behavior are more important and have to be reflected by the model to obtain realistic results.

A low energy release rate is necessary to obtain brittle fracture (and avoid ductile behavior). As a result energy dissipation through crack propagation appears to be insignificant. However, the energy release rate of ice is subject of ongoing discussion. It is also expected to be size dependent [31]. This is in contrast to other ice material properties, which have been studied extensively and can be applied with more confidence. Additionally, the interaction between the single surface contact algorithm and the penalty-based compression of the CZ elements has not been investigated to the full extent. The advantages and disadvantages of the CZM are listed in the following Table 4.

Table 4: Advantages and disadvantages of the CZM

Advantages:	Disadvantages
<ul style="list-style-type: none"> ▪ Volume-preserving ▪ Somewhat arbitrary fracture paths ▪ phenomenological model ▪ Few material parameters required 	<ul style="list-style-type: none"> ▪ Interaction with contact algorithm ▪ Increase of degrees of freedom ▪ Small simulation time step necessary ▪ Artificial compliance of CZ elements ▪ Still small loss of mass during element erosion

In the future, some improvements are necessary for a confident application of the CZM to ice-structure interaction problems. The cohesive model should consider hydrostatic stress to realistically reflect ice fracture. For the bulk material model, softening due to micro fracture and recrystallization should be included. Lastly, LS-Opt could be used to optimize material parameters. This is expected to work well for specific cases with known boundary conditions.

6 Summary

A cohesive model for brittle ice-structure interaction problems is presented. Basic problems of the CZM method are discussed. Recommendations for model generation are developed. The results are satisfactory for problems dominated by a single crack. A reliable simulation of complex ice-structure interaction problem is currently only possible in individual cases, which are not dominated by continuous crushing processes. Despite these limitations, ice-structure interaction scenarios are successfully simulated. Open questions remain regarding material behavior (e.g. friction) and the contact algorithms. These problems were particularly evident in the case of the rigid plate. Overall, this research is seen as a first step and further validation is needed, especially for varying geometric scales and different problems, e.g. with confined specimens.

7 Acknowledgment

This work was supported by the US Office of Naval Research Global (ONRG) under NICOP Grant N62909-18-1-2127. We would also like to thank the German Federal Ministry for Economic Affairs and Energy (BMWi) for funding this research under the project reference number 0324022B and acknowledge the financial support of the Lloyd's Register Foundation within the "Joint Research Centre of Excellence for Arctic Shipping and Operations". Lloyd's Register Foundation helps to protect life and property by supporting engineering-related education, public engagement and the application of research. It is stated that all funders are not responsible for any of the content of this publication.

8 References

- [1] V.-G. Schulze, *Arktisstrategien Überblick 2017*, 2017.
- [2] BMWi, *Eckpunkte für die Reform des EEG*, 2014.
- [3] L. Kellner, H. Herrnring, M. Ring, *REVIEW OF ICE LOAD STANDARDS AND COMPARISON WITH MEASUREMENTS*, Proceedings of the ASME 2017 36 th International Conference on Ocean, Offshore and Arctic Engineering (2017).
- [4] B. Erceg, R. Taylor, S. Ehlers, B.J. Leira, *A response comparison of a stiffened panel subjected to rule-based and measured ice loads*, San Francisco, 2014.
- [5] B. Quinton, C. Daley, D. Colbourne, R. Gagnon, *Experimental investigation of accidental sliding loads on the response of hull plating*, in: C. Guedes Soares (Ed.), *Progress in the Analysis and Design of Marine Structures*, CRC Press, Milton, UNKNOWN, 2017, pp. 513–522.
- [6] P.F. Moore, I.J. Jordaan, R.S. Taylor, *Explicit finite element analysis of compressive ice failure using damage mechanics*, 2013.
- [7] A. Gürtner, *Experimental and Numerical Investigations of Ice-Structure Interaction*. Doctoral thesis, Trondheim, 2009.
- [8] J. Kuutti, K. Kolari, P. Marjavaara, *Simulation of ice crushing experiments with cohesive surface methodology*, *Cold Regions Science and Technology* 92 (2013) 17–28.
- [9] H. Daiyan, B. Sand, *Numerical Simulation of the Ice-Structure Interaction in LS-DYNA*, 8th European LS-DYNA Users Conference, Strasbourg - May 2011 (2011).
- [10] D. Hilding, J. Forsberg, A. Gürtner, *Simulation of Loads from Drifting Ice Sheets on Offshore Structures*, 12. International LS-Dyna User Conference (2012).
- [11] G. Barenblatt, *The Mathematical Theory of Equilibrium Cracks in Brittle Fracture*, in: H.L. Dryden, T. von Karman (Eds.), *Advances in applied mechanics*, Academic P, New York, 1962, pp. 55–129.
- [12] D. Dugdale, *Yielding of steel sheets containing slits*, *Journal of the Mechanics and Physics of Solids* 8 (1960) 100–104.
- [13] K.-H. Schwalbe, I. Scheider, A. Cornec, *Guidelines for applying cohesive models to the damage behaviour of engineering materials and structures*, Springer, Heidelberg, New York, 2013.
- [14] C. Dávila, P. Camanho, *Decohesion Elements using Two and Three-Parameter Mixed Mode Criteria*, in: *American Helicopter Society Conference*, 2001.
- [15] LSTC, *LS-DYNA Keyword User's Manual: Volume II Material Models*, 2017.
- [16] A. Tabiei, W. Zhang, *Cohesive element approach for dynamic crack propagation: Artificial compliance and mesh dependency*, *Engineering Fracture Mechanics* 180 (2017) 23–42.
- [17] M. Falk, A. Needleman, J. Rice, *A critical evaluation of cohesive zone models of dynamic fracture*, *J. Phys. IV France* 11 (2001) Pr5-43-Pr5-50.
- [18] A. Turon, C. Dávila, P. Camanho, J. Costa, *An engineering solution for mesh size effects in the simulation of delamination using cohesive zone models*, *Engineering Fracture Mechanics* 74 (2007) 1665–1682.
- [19] C.E. Renshaw, N. Golding, E.M. Schulson, *Maps for brittle and brittle-like failure in ice*, *Cold Regions Science and Technology* 97 (2014) 1–6.
- [20] A. Palmer, K. Croasdale, *Arctic offshore engineering*, World Scientific Pub, Singapore, Hackensack, NJ, 2013.
- [21] E.M. Schulson, P. Duval, *Creep and fracture of ice*, Cambridge Univ. Press, Cambridge, 2009.
- [22] H.W. Liu, K.J. Miller, *Fracture Toughness of Fresh-Water Ice*, *J. Glaciol.* 22 (1979) 135–143.
- [23] G.D. Ashton (Ed.), *River and lake ice engineering*, Water Resources Publications, Littleton, Colo., 1986.
- [24] P.V. Hobbs, *Ice physics*, Oxford Univ. Press, Oxford, 2010.
- [25] J.H. Currier, E.M. Schulson and W.F. St. Lawrence, *A study on the tensile strength of ice as a function of grain size*, 1983.

- [26] R. Frederking, O.J. Svec, G.W. Timco, On measuring the shear strength of ice, in: S. Hiroshi, H. Ken-ichi (Eds.), Proceedings of The 9th International Symposium on Ice, Sapporo, 1988, pp. 76–88.
- [27] Y. Wei, S.J. DeFranco, J.P. Dempsey, Crack-fabrication techniques and their effects on the fracture toughness and CTOD for fresh-water columnar ice, *J. Glaciol.* 37 (1991) 270–280.
- [28] N. Fletcher, *The chemical physics of ice*, Cambridge U.P, London, 1970.
- [29] H. Herrring, J.M. Kubiczek, S. Ehlers, N. Niclasen, M. Burmann, Experimental investigation of an accidental ice impact on an aluminium high speed craft, Proceedings of the 6th International Conference on Marine Structures (MARSTRUCT 2017) (2017) 697–704.
- [30] E.M. Schulson, A.L. Fortt, Friction of ice on ice, *J. Geophys. Res.* 117 (2012) n/a-n/a.
- [31] A. Fantilli, B. Chiaia, B. Frigo, Analogies in Fracture Mechanics of Concrete, Rock and Ice, *Procedia Materials Science* 3 (2014) 397–407.